Since January 2020 Elsevier has created a COVID-19 resource centre with free information in English and Mandarin on the novel coronavirus COVID-19. The COVID-19 resource centre is hosted on Elsevier Connect, the company's public news and information website.

Journal of Proteomics 222 (2020) 103802

Contents lists available at ScienceDirect

Journal of Proteomics

journal homepage: www.elsevier.com/locate/jprot

Glycoproteome in silkworm *Bombyx mori* and alteration by BmCPV infection

Feifei Zhu[a,b], Dong Li[a], Dandan Song[a], Shuhao Huo[b], Shangshang Ma[a], Peng Lü[a], Xiaoyong Liu[a], Qin Yao[a], Keping Chen[a,*]

[a] Institute of Life Sciences, Jiangsu University, Zhenjiang 212013, China
[b] School of Food and Biological Engineering, Jiangsu University, Zhenjiang 212013, China

ARTICLE INFO

Keywords:
Silkworm
Bombxy mori
Glycoproteome
O-glycans
BmCPV

ABSTRACT

The biological functions of protein glycosylation have been increasingly recognized but not yet been very well understood, especially in lower organisms. Silkworm as a model lepidopteran insect and important economic insect, has been widely studied in life science, however, the current knowledge on the glycosylation status of its proteome is not satisfactory, and little is known about how pathogenic infections could affect the glycosylation status. This study performed large scale glycosite mapping for the silkworm *Bombyx mori* P50 strain, and quantitatively compared with that infected with the *Bombyx mori* cytoplasmic polyhedrosis virus (BmCPV). Some 400 glycoproteins were mapped in the silkworm, including N- and O-glycoproteins. Upon virus infection, the glycosylation levels of 41 N-glycopeptides were significantly changed, some of them belonging to transmembrane glycoproteins. The O-glycosylation profiles were also affected. In addition, 4 BmCPV-encoded viral proteins were found to be glycosylated for the first time, including polyhedrin, P101, VP3, and the NS protein. This study drafted a silkworm protein glycosylation map and underlined the potential impact of virus infection on glycosylation.

Significance: This study reveals the characteristics of the glycoproteome in the silkworm strain P50, and quantitatively compared to that infected by the virus BmCPV, which underlines the impact of virus infection on the alteration of protein glycosylation in invertebrate species. Our findings add to the knowledge of the post translational modifications of this model organism, and also uncovered for the first time the glycosylation status of the viral proteins expressed by BmCPV.

1. Introduction

Silkworm *Bombyx mori* is an economically important Lepidopteran insect. Since its genome revealed in 2004 [1], it has become an increasingly popular model organism for molecular biology [2]. However, compared to the current knowledge on the silkworm's genome and transcriptome, we do not know much at the proteomic level, especially the status of post translational modifications (PTMs) of the proteome. Glycosylation, being one of the most common and diverse PTMs, has been widely acknowledged in vertebrates as an important indicator of their physiological or pathological state [3], however, very little is known about how glycosylation are altered in lower organisms, like during a pathogen invasion. Such investigations can provide clues to the interactions between glycosylation pathways, inflammatory responses and viral immune escape [4].

The initial steps of viral infections always involve the attachment of viral particles to the receptors on the host cell surface. An important class of the receptors is transmembrane glycoproteins, which play vital roles cell adhesion and receptor bindings [5]. Therefore, glycosylation patterns of the host cell, especially on the cell surface, can influence the interactions between an infecting virus and the host, and identifying such molecules are critical to the understanding of viral infection mechanisms and host immune responses. Once a virus enters the host cell, it hijacks the host's cellular machinery for viral replication, altering numerous biological pathways of the cell, which is evidenced by changes in the expression levels of many genes, transcripts, and proteins. Although several studies have performed transcriptomic and proteomic comparisons on the silkworm upon virus infection, such as by the *Bombyx mori* cytoplasmic polyhedrosis virus (BmCPV) [6,7], whether the glycosylation profiles are affected have not been reported.

BmCPV is one of the earliest identified viruses infecting silkworms, and often results in significant economic loss to the sericulture industry. BmCPV is a double stranded RNA virus belonging to the *Cypovirus* genus, *Reoviridae* family. Its genome contains 10 discrete copacked RNA segments [8], but only a few of them has been cloned and characterized so far [9,10]. The RNA genome is wrapped by 5 structural proteins,

* Corresponding author.
E-mail address: kpchen@ujs.edu.cn (K. Chen).

https://doi.org/10.1016/j.jprot.2020.103802
Received 18 March 2020; Received in revised form 19 April 2020; Accepted 27 April 2020
Available online 29 April 2020

namely VP1–5 [11]. The virus forms occlusion bodies in infected silkworm midgut, which is composed of the matrix protein polyhedrin that encloses many visions within the matrix [12].

In this study, we performed large scale glycosylation site mapping on the silkworm strain P50, and quantitatively compared to that infected by BmCPV. The mapping strategy, which was first introduced by Zielinska et al. [13], uses high precision mass spectrometer for detection of a + 2.988 Da mass shift after enzymatic deamidation of the N-glycosylated asparagine residue in O^{18} water. Taking advantage of the greatly reduced glycosylation complexity due to removal of the N-glycans, we were also able to simultaneously map the O-glycosites and their associated glycans by searching against an insect O-glycan panel. Additionally, the glycosylation profile of the virus-encoded proteins were obtained. Transmembrane glycoproteins and significantly regulated glycoproteins upon virus infection were marked, which provides clues for future investigation of the role of glycosylation during viral infection in invertebrate systems.

2. Experimental procedures

2.1. Silkworm breeding and viral administration

The silkworm P50 strain was obtained from the Institute of Life Sciences, Jiangsu University, and the BmCPV virus was graciously given by Prof. Chengxiang Hou at the Sericultural Research Institute, Chinese Academy of Agricultural Sciences, Zhenjiang. The silkworm were reared on fresh mulberry leaves at 25 ± 1 °C and 70–90% relative humidity. On the first day of 5th instar, the silkworm was fed with 5 μL of BmCPV virion at 10^8 polyhedra/mL in phosphate buffered saline (PBS), and the control larvae were fed with PBS. After 72 h, silkworms were harvested and residual mulberry leaves were removed from the gut and then preserved at −80 °C. Biological triplicates in each group were prepared for the following sample processing and analysis.

2.2. Protein extraction and digestion

To the silkworm sample, 1.5 mL SDT lysis buffer containing 4% SDS, 100 mM Tris/HCl, and 0.1 M DTT at pH 7.6 was added, and the sample was homogenized in a tissue lyser (Shanghai Jingxin Co., Shanghai, China) using three beating cycles at 120 Hz, 60 s at 4 °C. The solution was then sonicated in an ice bath for 10 min, boiled for 15 min, and then centrifuged at 14000*g* for 40 min. The supernatant was collected and the protein concentration was determined by Bradford analysis (ThermoFisher scientific) and stored at −80 °C for further use.

The protein extract was aliquoted to a tube containing 400 μg of total protein and was boiled for 5 min, cooled to room temperature, and then mixed with 200 μL of UA buffer (8 M urea, 150 mM Tris HCl, pH 8.0). The mixture was transferred to a 10 kD ultrafiltration tube (Merck Millipore) and centrifuged at 14000*g* at 4 °C for 15 min. The filtrate was discarded and this step was repeated before 100 μL of 100 mM iodoacetamide (IAA) in UA buffer was added. After mixing at 600 rpm for 1 min, the samples were incubated for 20 min in darkness. The filters were washed three times with UA buffer at 14000*g*, 4 °C for 15 min, then 100 μL of 25 mM NH_4HCO_3 were added to the filter and the sample was centrifuged for 15 min under the same conditions. This step was repeated twice. Trypsin was added at a ratio of trypsin: protein = 1:50 to the samples and gently mixed for 1 min, and then incubated at 37 °C for 16 h. The filtrate was then collected by centrifugation. The filter was washed with 40 μL 25 mM NH_4HCO_3 and the filtrate was combined.

2.3. Glycopeptide enrichment, O18 deamidation, and LC-MS analysis

The digested peptides was transferred to a new 10 kD filter and mixed with 100 μL lectin mixture containing 2.5 mg/mL Con A, 2.5 mg/mL WGA, and 0.8 mg/mL RCA in buffer A (buffer A = 1 mM $CaCl_2$, 1 mM $MnCl_2$, 0.5 M NaCl in 20 mM Tris-HCl, pH 7.3). After gentle mixing at 600 rpm for 1 min, the mixture was incubated at room temperature for 1 h and then centrifuged at 14000 *g* for 10 min. The samples were washed by 200 μL buffer A three times. Afterwards, 50 μL of 25 mM NH_4HCO_3 in $H_2{}^{18}O$ was added to precondition the filter and discarded by centrifugation. This step was repeated twice. The filter was placed in new collection tube and 40 μL PNGase F (500 units) in 25 mM NH_4HCO_3 made in $H_2{}^{18}O$ was added to the filter and the samples were incubated for 3 h at 37 °C. The deglycosylated (or deamidated) peptides were eluted by centrifugation and the filter was washed with 25 mM NH_4HCO_3 in $H_2{}^{18}O$ twice and the elution was combined. The samples were then desalted using a Zip-Tip (Merck Millipore) protocol according to the manufacture's protocol and ready for LC-MS analysis.

The deamidated peptides were loaded onto an Acclaim PepMap100 sample concentrating column (100 μm × 2 cm, Thermo Scientific) and then separated by an C18 capillary column (75 μm × 10 cm, 3 μm). Buffer A contained 0.1% formic acid in water and buffer B was 0.1% formic acid in 84% acetonitrile. The peptide sample was separated at a flow rate of 250 nL/min using a 2 h gradient. MS analysis was performed on a LTQ-Orbitrap Velos mass spectrometer (Thermo Fisher). After each full scan, top ten intense precursor ions were isolated and fragmented using HCD at an isolation window of 2 *m/z* and normalized collision energy of 30 eV.

2.4. Data analysis

LC-MS raw data were directed processed by Peaks Studio software (Bioinformatics Solutions Inc.) for identification of proteins and post translational modifications as described previously [14]. Briefly, Silkworm reference proteome (Uniprot ID UP000005204) was used as the protein database, and the parameters used for database searching was: 10 ppm as parent mass tolerance, 0.1 Da as fragment mass tolerance, 2 missed cleavages for tryptic digestion, carbamidomethyl as the fixed modification, methionine oxidation, protein N-terminal acetylation, and asparagine deamidation (+2.988 Da) as the variable modifications. For post translational modifications (PTMs), a series of 38 O-glycan compositions (Table S1) were set as the variable modifications to the threonine or serine residues. A maximum of 5 PTMs were allowed per peptide. The results were further filtrated using the following parameters: de novo average localized score ≥ 50%, unique peptide ≥2, PTM Ascore ≥20, and false discover rate ≤ 1%. For quantitative analysis, Perseus software [15] was used for further data processing and visualization. Briefly, the raw intensities obtained by Peaks software were transformed using natural log, and those had at least two valid intensities among the triplicate in at least one group (control or infected) were retained, and the remaining missing values were replaced with normal distribution (width = 0.3; downshift = 2.6). Student's *t*-test was performed to obtain statistically different ($p < .05$) (glyco) peptides between the groups. Gene ontology enrichment was performed using the ShinyGo webserver [16]. Transmembrane topology was predicted using the Phobius web server [17].

3. Results and discussion

3.1. Viral glycoprotein expression in the BmCPV-infected P50 group

Viral glycoproteins play important roles in virus attachment, penetration and uncoating, and serve as a protective shield from the host immune systems [18,19]. Alteration of the glycans on the virus particle can alter the virulence and change the host range [20–22]. Therefore, profiling the glycosylation of virus-encoded proteins are necessary to the functional characterization the protein as well as to the understanding of the mechanisms of viral infection. The glycosylation status of BmCPV viral proteins have not been explored to date. In this study, effective viral propagation in the silkworm was confirmed by

Table 1
N-glycoproteins encoded by the BmCPV virus.

Protein ID	Protein names	M.W. (kDa)	N-glycosites
B8YCR2	Polyhedrin	28.5	N77
C6K2M9	NS Protein	44.3	N69,N48,N138
C7EWL8	P101	101.0	N684
D3JWE7	VP3	120.0	N801

expression of the viral proteins in the host body. In the total glycoproteome of the virus-infected silkworm, 4 N-glycoproteins were found to be BmCPV-encoded, whereas no O-glycosylation was detected (Table 1). These viral glycoproteins were not found in the control P50 group.

Polyhedrin, encoded by the genome segment 10 of the BmCPV virus and organized in octameric or dodecameric forms [23], is the major matrix protein surrounding the virus envelope and protects the virions against long term harsh environments. Polyhedrin has typical molecular weight of 27–31 kDa, but no significant sequence similarities were found between the polyhedrins derived from the CPVs of different host species [9,24,25]. While baculovirus polyhedrin has been found with glycosylation potential [23], there has been controversy on whether the cypovirus polyhedrin is glycosylated or not. It has been previously suggested to be glycosylated based on positive color-reactions with acid-Schiff reagent [11], however, molecular cloning of this protein showed that polydedrin does not contain a transmembrane signal peptides which guide peptide glycosylation [9]. In this study, glycosite mapping showed that BmCPV polyhedrin is N-glycosylated at the single site N77, confirming that it is a glycoprotein, and it is speculated that the sugar coating could further enhance the stability and protection of the virion. Another glycoproteins P101, which is a 101 kDa protein encoded by the genome segment 5, was identified with a single glycosylation site at N684, although this protein was predicted with three possible N-glycosylation sites based on motif analysis [26]. The other two viral glycoproteins were VP3, a capping protein [8], which was glycosylated at N801 and the non-structural (NS) protein, which was mapped with three glycosylation sites at N69, N48, and N138. The functions of these viral proteins have not been clarified or experimentally validated so far, and even less is known about what their glycosylation does for these proteins during virus infections. Therefore, it would be of great interest to investigate these glycosylated viral proteins and their roles during virus infection.

3.2. Characteristics of the P50 silkworm N-glycoproteome

A total of 762 N-glycopeptides belonging to 389 N-glycoproteins were identified in the P50 control and BmCPV-infected groups (Table S2), revealing a high level of glycosylation in this lepidopteran insect. More than 95% of the mapped glycoproteins were within 200 kDa, and a significant portion of them were closely resided within 10–100 kDa (Fig. 1a). The N-glycoproteins were predominantly singly or doubly glycosylated, although 14 of them were mapped with more than 5 glycosites per protein (Fig. 1b). Fig. 1c showed that all the 762 identified glycosylation site has the consensus sequence N-X-T/S, demonstrating the highly conserved motif required for N-glycosylation. Among the 389 identified N-glycoproteins, 118 were predicted to be transmembrane glycoproteins (Table S3), which can be interesting candidates to explore as potential cell surface receptors to outside pathogens. The total glycoproteins identified in the silkworm were analyzed by gene ontology (GO) enrichment in the category of biological process, indicating that the silkworm glycoproteome mainly involve in metabolic processes, cell adhesion, and proteolysis processes (Fig. 1d).

Table 2 lists the top 20 most abundant N-glycoproteins in the P50 silkworm. The silkworm storage protein is the most abundant glycoprotein in the P50 silkworm. It plays important roles in insect metamorphosis and development, and may involve in the innate immune response to pathogens [27,28]. Previous study indicated that it is a glycoprotein [29], but the specific sites were not known. In this study, the storage protein is mapped with three N-glycosites at N208, N519, and N598. The second most abundant silkworm N-glycoprotein is a putative cuticle protein glycosylated at N66. Although many insect cuticle proteins were found to be glycosylated [30], the functions of these modifications are not yet clear. The protein containing the highest number of glycosite was H9JRT0, with 10 N-glycosites, and was the eighth most abundant N-glycoprotein. However, it has not been characterized at the protein level. As Table 2 shows, a lot of the glycoproteins are “uncharacterized”, thus continued effort are needed to investigate their structures and functions, including their glycosylation status.

3.3. Quantitative comparison of the N-glycoproteomes between control and BmCPV-infected P50 strains

To understand how protein glycosylation status is affected by viral infection, the total glycoproteomes in the P50 control and BmCPV-infected groups were analyzed and compared. For reliable quantitative comparison between the glycoproteomes, the data were further filtered retaining those detected at least twice in the triplicate in at least one group. This yields 489 glycopeptides belonging to 287 glycoproteins (Table S4), which were then used for quantitative comparison between the control and BmCPV-infected group. The glycopeptide intensities within each group are highly replicable (Fig. 2a), as demonstrated by low discrepancy in intensity between the replicates. Majority of the glycopeptide intensities in the replicates were within 10% from each other.

A heat map was constructed to compare the identified glycopeptides in the two groups (Fig. S1), which showed that majority of the N-glycopeptides had a similar profile between the control and the virus-infected groups. Statistically significant ($p < .05$) glycopeptides between the two groups were shown in Fig. 2c and d. A total of 14 glycopeptides were significantly downregulated in the virus-infected group, and another 27 glycopeptides significantly upregulated. Among them, 9 were predicted transmembrane proteins (Table S3). These 41 differentially regulated glycoproteins were categorized in metabolic processes, cell adhesion as well as in response to stimulus (Fig. 2b), indicating a change of molecular interactions by the virus infection. There have been evidences that pathogens can hijack host's glycosylation system to manipulate immune responses to the advantage of the pathogen [4]. Thus, the changes in the glycosylation level can modulate cellular and molecular functions, which is likely for the purpose of increasing the host susceptibility to the infection. Again, a lot glycoproteins were uncharacterized, and further investigations on these proteins may be necessary and insightful for understanding the molecular mechanisms during the virus infection.

Among the 14 downregulated glycopeptides, the signal sequence receptor (SSR, Q2F5L0) showed the most significant difference ($p = 2.5 \times 10^{-6}$) (Fig. 2c). SSR is an integral, glycosylated protein of the rough ER membrane and mediates the translocation of a peptide across the ER membrane [31]. The significant downregulation of SSR indicates that BmCPV infection may induce ER stress and influence the glycosylation level of SSR as a part of the ER stress response.

The significantly upregulated glycopeptides include several enzyme classes such as oxidases and peptidases, and several other proteins including DNA supercoiling factor, serpin, and integrin beta (Fig. 2d). Among these, integrin beta are a family of evolutionarily conserved transmembrane glycoproteins that mediate bidirectional transmembrane signaling and cell to cell interactions, and are important in many physiological and pathological processes [32]. Previous studies showed that silkworm integrin beta interacts with the BmCPV virion, and that silencing integrin beta gene could inhibit viral infection to the silkworm [33]. Our data showed that integrin beta was upregulated during

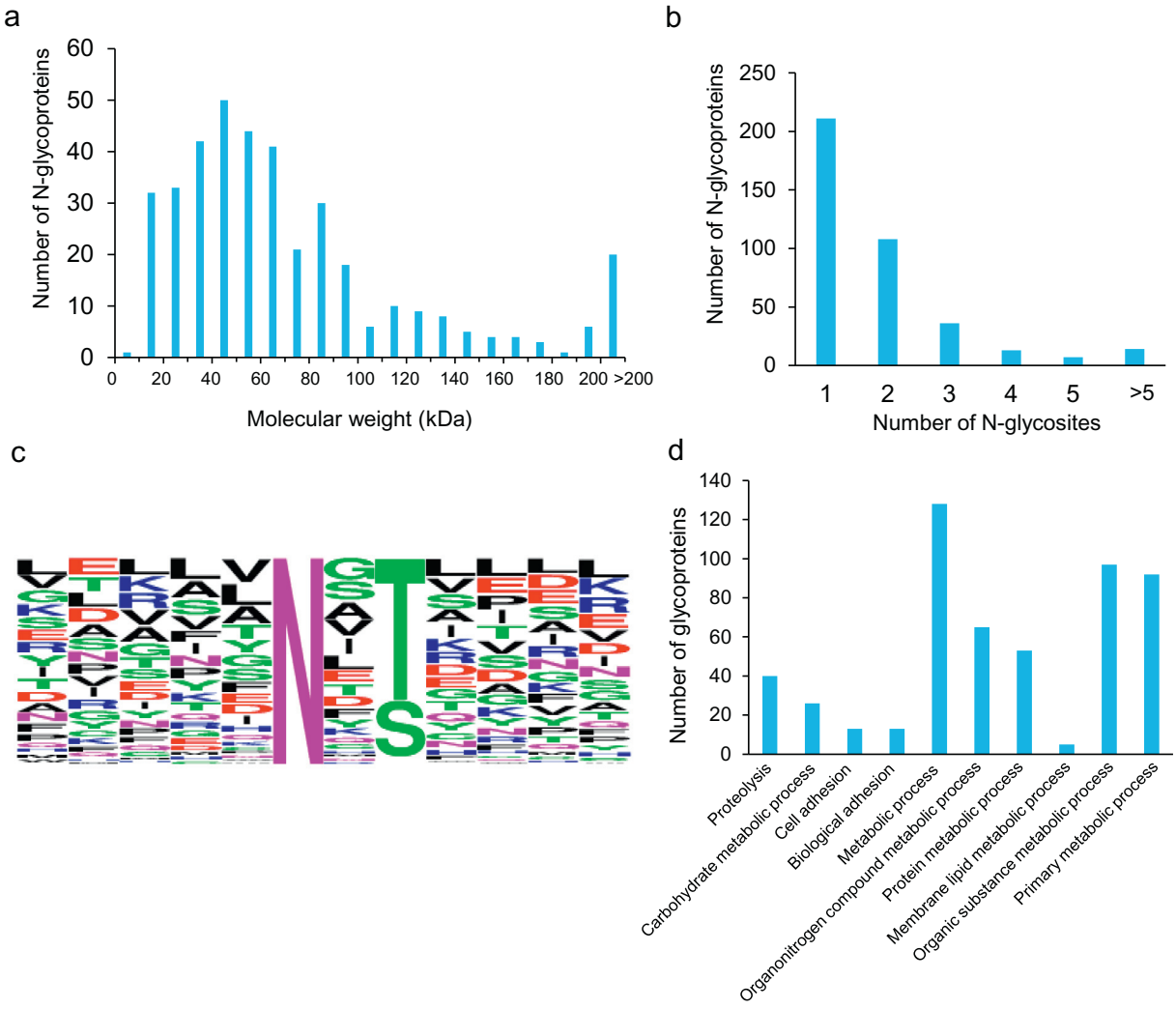

Fig. 1. Characteristics of the silkworm N-glycoproteome. (a) Molecular weight distribution of silkworm N-glycoproteins in the P50 strain, (b) distribution of the number of N-glycoproteins having a particular number of N-glycosites, (c) sequence motif analysis centered on the N-glycosylation site, and (d) top10 enriched GO terms in biological processes ($p < .05$) for the 389 total glycoproteins identified in silkworm.

Table 2
Top 20 most abundant N-glycoproteins in the silkworm P50 strain.[a]

Protein ID	Protein names	M.W. (kDa)	N-glycosites	Gene names
H9JHM9	Silkworm storage protein	82.8	N208, N519, N598	sp3
C0H6L5	Putative cuticle protein	12.6	N66	BmorCPR24
H9J9M0	Chitin-binding type-2 domain-containing protein	61.4	N244, N296, N274, N300	101,740,647
H9J8C7	Uncharacterized protein	16.4	N51, N67	
H9J9M1	Uncharacterized protein	65.3	N330	
H9J1A5	SERPIN domain-containing protein	44.4	N23, N140, N334	
H9JPK1	Uncharacterized protein	58.0	N93	101,736,296
H9JRT0	Uncharacterized protein	425.7	N43, N959, N1164, N1385, N2105, N2374, N2688, N2745, N2866, N3597,	
H9JWX6	Collagen IV NC1 domain-containing protein	178.1	N16, N220	
H9JIA9	Uncharacterized protein	22.2	N80	
H9JPG9	Transferrin	71.7	N318	
G9FL14	DNA supercoiling factor	38.0	N177	LOC692759
Q9XXV0	Phenoloxidase-activating enzyme	48.0	N239, N334	PPAE
H9JRS9	SEA domain-containing protein	40.5	N225, N138	
H9J1S1	Uncharacterized protein	78.9	N130, N315, N591	
H9JTG9	Aldo-keto reductase AKR2E4	34.4	N161	akr2e
H9JRR1	Uncharacterized protein	81.1	N170, N345, N463, N534	
H9JB73	Uncharacterized protein	23.8	N111	
H9J1X5	Uncharacterized protein	57.1	N43, N237	
H9JXY5	Uncharacterized protein	44.7	N202, N317	101,741,915

[a] Based on the average intensity of its most abundant N-glycopeptides.

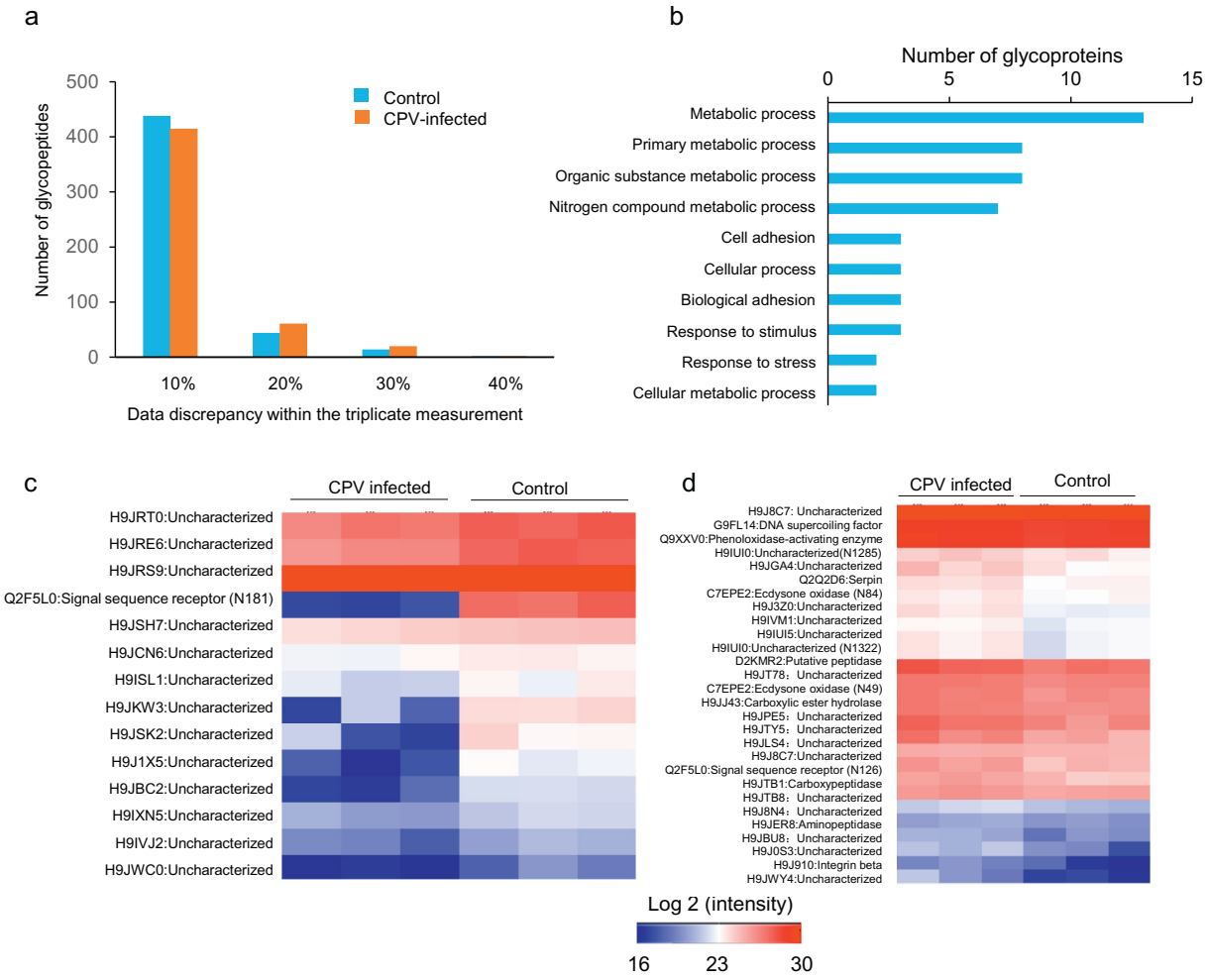

Fig. 2. Quantitative comparison between the N-glycoproteomes of the control and virus-infected groups. (a) Data discrepancy of the glycopeptide intensities within the triplicate measurement for each group, (b) GO analysis in terms of biological process for the 41 differentially regulated glycoproteins upon BmNPV infection, the heat maps of the (c) significantly downregulated and (d) significantly upregulated N-glycopeptides between the control and BmCPV-infected P50 strains.

BmCPV infection, indicating its potential role as a cell adhesion receptor facilitating viral propagation. Sepin, a glycosylated serin protease inhibitor, was previously found significantly upregulated in the bacteria-infected fat body of the silkworm [34], similar to what we observed in the silkworm upon viral infection in this study.

It is noted that the ecdysone oxidase and another glycoprotein (H9IUI0) both contain two glycopeptides that were downregulated. However, another interesting observation is that while the glycopeptide (N181) of SSR was downregulated, its glycopeptide at N126 wass upregulated. The results indicate that while viral infection affects the level of protein glycosylation, it may or may not influence in the same way. Therefore, to evaluate or compare the profiles of multiply glycosylated proteins, it is necessary to locate individual glycopeptides instead of the glycoprotein as a whole, because each glycosylation site might change independently from the rest of the glycosylation sites upon perturbation or stimuli.

3.4. O-glycan profiles of the control and BmCPV-infected P50 silkworms

Unlike N-glycosylation, O-glycosylation sites do not have a consensus sequence, and deglycosylation could not be achieved by a universal enzyme currently. Due to the high diversity of O-glycosylation and its close association with various pathological and physiological states, the ability to reveal the O-glycans and their attached sites, especially in a large scale, becomes very demanding. In this study, due to the deamidation process that removes the N-glycans from the peptide, the workload for database searching was greatly reduced, which makes it possible to perform large scale O-glycosylation mapping at the same time during N-glycosite mapping.

The O-glycosylation mapping results for the P50 control and virus-infected groups were shown in Table 3. Only those identified at least twice in the triplicate were retained for comparison purposes. A total of 13 O-glycoproteins were mapped in the P50 and its BmCPV-infected strains. The most frequently occurred O-glycans were fucose (F) and HexNAc (N), followed by Hex1HexNAc2 (H1N2), HexNAc2 (N2), HexNAc3 (N3) and HexHexNAcFuc (H1N1F1). A lot of the O-glycoproteins are also N-glycosylated (Table 3). It was noticed that the uncharacterized protein H9IXN5 contain a surprisingly large number of N-glycosite: a total of 20, in addition to the O-glycosite identified (Table 3). A protein coverage map with its supporting peptides for this unknown but interesting protein was shown in Fig. S2, demonstrating a reliable glycosite mapping of this protein.

Myosin regulatory light chain (RLC), an important structural element of myosin, is critical to cell movement and muscle contractions. RLC is a well-known phosphoprotein and its dynamic phosphorylation state is tissue-specific and case-specific [35,36]. However, it has not been reported to be glycosylated before. In this study, silkworm RLC was found to be O-fucosylated at S104, S121 or S124, depending on whether the silkworm was infected with the virus or not. The silkworm larval cuticle protein LCP-17 was found to be N-glycosylated at N52 and

Table 3
O-glycosylation profiles of control and BmCPV-infected P50 silkworms.[a]

Protein ID	Protein names	M.W. (kDa)	N-glycosites	O-glycosites (glycan)	
				Control	CPV-infected
H9JXG1	Uncharacterized protein	123.6	N152	S824(H1N2)	S824(H1N2)
H9JRT0	Uncharacterized protein	425.7	N43, N959, N1164, N1385, N2105, N2374, N2688, N2745, N2866, N3597		T2673(N1)
H9IXN5	Uncharacterized protein	405.1	N177, N411, N908, N1035, N1260, N1317, N1689, N2015, N2091, N2114, N2241, N2276, N2341, N2451, N2491, N2759, N3024, N3097, N3109, N3525	T1905(H1)	
H9J6Y6	Uncharacterized protein	15.8	N72	T70(F1); S71(F1)	T70(F1); S71(F1)
H9JHM9	Silkworm storage protein	82.8	N208, N519, N598		S210(F1)
O02387	Larval cuticle protein LCP-17	15.3	N52, N97	S104(N1)	
H9JTY5	Uncharacterized protein	69.3	N403		S412(N3)
H9J9M1	Uncharacterized protein	65.3	N330	T151(N1)	T151(N1)
Q1HPS0	Myosin regulatory light chain 2	22.0		S104(F1); S124(F1)	S121(F1)
H9J9M0	Chitin-binding type-2 domain-containing protein	61.4	N244, N296, N274, N300		S295(H1)
H9JTA0	Dynein light chain	10.4			S14(N2)
H9J609	Uncharacterized protein	100.2			S765(H1N1F1)

[a] The O-glycosites and glycans were detected at least twice among the triplicate.

N97 in both groups but only O-glycosylated in the control group at site S104 (Table 3). On the other hand, the silkworm storage protein (H9JHM9) and the uncharacterized proteins H9JRT0, H9JTY5, H9J9M0, H9JTA0, and H9J609 were not detected with O-glycosylation in the control, but were found with O-glycosylation in the virus-infected group. The glycosylation profiles of the proteins H9JXG1, H9J9M1 and H9J6Y6, all of which are uncharacterized proteins, remain unchanged after virus infection.

Previously, we have characterized the glycoproteome for two other silkworm strains, 306 and NB. By comparing to the current study, it was noticed that the arylphorin protein, a type of the storage proteins, was heavily O-glycosylated in the 306 and NB strains [14], however, it was not being modified by O-glycosylation in the P50 strain, neither in the control nor BmCPV-infected groups. The silkworm storage protein (H9JHM9), myosin regulatory light chain 2 (Q1HPS0), and several other uncharacterized proteins (H9JRT0, H9JXG1, H9J9M0) were found to be O-glycosylated in all P50, 306 and NB strains, although the glycosylation site and glycan profiles were somewhat different (Table S5). The changes in glycosylation states, together with other molecular differences such as genetic mutations, may contribute to the different responses these strains develop to virus invasions.

It has been well established that alteration of glycosylation is closely associated with changes in physiological and pathological states. Our previous study also showed that baculovirus resistant and susceptible silkworm strains were differentially glycosylated [14]. Combining the results from this study, which showed that viral infection altered protein glycosylation in the silkworm, the relationships between host glycosylation and virus/microbe infection can be intertwined: 1) host glycosylation changes lead to infection and inflammation, 2) infection and inflammation lead to host glycosylation changes, which leads to molecular and cellular functional differences.

Glycosylation modification is highly dynamic and can be affected by many cellular factors and processes. During BmCPV infection, the silkworm's cellular machinery was hijacked and many biological pathways were altered, including the glycosylation pathway. In this study, the total glycoproteome in the silkworm P50, including the N- and O-glycosylation status was uncovered. Some 400 N- and O-glycoproteins were confidently mapped, including 118 transmembrane glycoproteins, indicating a rich, complex and yet much unknown glycoproteome. Quantitative comparison showed that the glycosylation levels of about 40 proteins, including the transmembrane glycoproteins signal sequence receptor and integrin beta, were significantly changed after the virus infection. These glycoproteins are therefore of particular interest to study the relation between glycosylation level, inflammatory responses, and the virus immune escape. Additionally, four proteins encoded by the BmCPV genome were mapped with N-glycosylation, revealing for the first time the glycosylation status of the BmCPV-encoded viral proteins.

Declaration of Competing Interest

None.

Acknowledgement

This work was supported by the National Natural Science Foundation of China (31702186, 31861143051 and 31872425), and China Postdoctoral Science Foundation (2016M601725).

Appendix A. Supplementary data

Supplementary data to this article can be found online at https://doi.org/10.1016/j.jprot.2020.103802.

References

[1] Q. Xia, Z. Zhou, C. Lu, D. Cheng, F. Dai, B. Li, P. Zhao, X. Zha, T. Cheng, C. Chai, et al., A draft sequence for the genome of the domesticated silkworm (bombyx mori), Science 306 (5703) (2004) 1937–1940.
[2] X. Meng, F. Zhu, K. Chen, Silkworm: a promising model organism in life science, J. Insect Sci. (2017) 17(5).
[3] C. Reily, T.J. Stewart, M.B. Renfrow, J. Novak, Glycosylation in health and disease, Nat. Rev. Nephrol. 15 (6) (2019) 346–366.
[4] L.S. Kreisman, B.A. Cobb, Infection, inflammation and host carbohydrates: a glycoevasion hypothesis, Glycobiology 22 (8) (2012) 1019–1030.
[5] A. Varki, Biological roles of glycans, Glycobiology 27 (1) (2016) 3–49.
[6] K. Gao, X.Y. Deng, M.K. Shang, G.X. Qin, C.X. Hou, X.J. Guo, Itraq-based quantitative proteomic analysis of midgut in silkworm infected with bombyx mori cytoplasmic polyhedrosis virus, J. Proteomics 152 (2017) 300–311.
[7] A. Kolliopoulou, F. Van Nieuwerburgh, D.J. Stravopodis, D. Deforce, L. Swevers, G. Smagghe, Transcriptome analysis of bombyx mori larval midgut during persistent and pathogenic cytoplasmic polyhedrosis virus infection, PLoS One 10 (3) (2015) e0121447.
[8] P. Mertens, The dsrna viruses, Virus Res. 101 (1) (2004) 3–13.
[9] M. Arella, C. Lavallée, S. Belloncik, Y. Furuichi, Molecular cloning and characterization of cytoplasmic polyhedrosis virus polyhedrin and a viable deletion mutant gene, J. Virol. 62 (1) (1988) 211.
[10] L. He, X. Hu, M. Zhu, Z. Liang, F. Chen, L. Zhu, S. Kuang, G. Cao, R. Xue, C. Gong, Identification and characterization of vp7 gene in bombyx mori cytoplasmic polyhedrosis virus, Gene 627 (2017) 343–350.
[11] C.C. Payne, J. Kalmakoff, Biochemical properties of polyhedra and virus particles of the cytoplasmic polyhedrosis virus of bombyx mori, Intervirology 4 (6) (1974)

354–364.
[12] S. Belloncik, H. Mori, Cypoviruses, in: L.K. Miller, L.A. Ball (Eds.), The Insect Viruses, 337-369 Springer US, Boston, MA, 1998.
[13] D.F. Zielinska, F. Gnad, J.R. Wiśniewski, M. Mann, Precision mapping of an in vivo n-glycoproteome reveals rigid topological and sequence constraints, Cell 141 (5) (2010) 897–907.
[14] F.F. Zhu, D. Li, D.D. Song, H.C. Xia, X.Y. Liu, Q. Yao, K.P. Chen, Precision mapping of n- and o-glycoproteins in viral resistant and susceptible strains of bombyx mori, J. Invertebr. Pathol. 167 (2019).
[15] S. Tyanova, T. Temu, P. Sinitcyn, A. Carlson, M.Y. Hein, T. Geiger, M. Mann, J. Cox, The perseus computational platform for comprehensive analysis of (prote)omics data, Nat. Methods 13 (9) (2016) 731–740.
[16] S.X. Ge, D. Jung, Shinygo: a graphical enrichment tool for ani-mals and plants, bioRxiv (2018) 315150.
[17] L. Käll, A. Krogh, E.L.L. Sonnhammer, Advantages of combined transmembrane topology and signal peptide prediction—the phobius web server, Nucleic Acids Res. 35 (suppl_2) (2007) W429–W432.
[18] A.C. Walls, M.A. Tortorici, B. Frenz, J. Snijder, W. Li, F.A. Rey, F. DiMaio, B.-J. Bosch, D. Veesler, Glycan shield and epitope masking of a coronavirus spike protein observed by cryo-electron microscopy, Nat. Struct. Mol. Biol. 23 (10) (2016) 899–905.
[19] A.M. Gram, T. Oosenbrug, M.F.S. Lindenbergh, C. Büll, A. Comvalius, K.J.I. Dickson, J. Wiegant, H. Vrolijk, R.J. Lebbink, R. Wolterbeek, et al., The epstein-barr virus glycoprotein gp150 forms an immune-evasive glycan shield at the surface of infected cells, PLoS Pathog. 12 (4) (2016) e1005550.
[20] R.C. Knoper, J. Ferrarone, Y. Yan, B.A. Lafont, C.A. Kozak, Removal of either n-glycan site from the envelope receptor binding domain of moloney and friend but not akv mouse ecotropic gammaretroviruses alters receptor usage, Virology 391 (2) (2009) 232–239.
[21] M.S. Maginnis, S.A. Haley, G.V. Gee, W.J. Atwood, Role of n-linked glycosylation of the 5-ht2a receptor in jc virus infection, J. Virol. 84 (19) (2010) 9677–9684.
[22] I. Fernandez-Sainz, L.G. Holinka, B.K. Gavrilov, M.V. Prarat, D. Gladue, Z. Lu, W. Jia, G.R. Risatti, M.V. Borca, Alteration of the N-linked glycosylation condition in e1 glycoprotein of classical swine fever virus strain Brescia alters virulence in swine, Virology 386 (1) (2009) 210–216.
[23] X. Ji, G. Sutton, G. Evans, D. Axford, R. Owen, D.I. Stuart, How baculovirus polyhedra fit square pegs into round holes to robustly package viruses, EMBO J. 29 (2) (2010) 505–514.
[24] F. Fossiez, S. Belloncik, M. Arella, Nucleotide sequence of the polyhedrin gene of euxoa scandens cytoplasmic polyhedrosis virus (escpv), Virology 169 (2) (1989) 462–465.
[25] M.S. Galinski, Y. Yu, B.R. Heminway, G.S. Beaudreau, Analysis of the c-polyhedrin genes from different geographical isolates of a type 5 cytoplasmic polyhedrosis virus, J. Gen. Virol. 75 (Pt 8) (1994) 1969–1974.
[26] K. Hagiwara, J. Kobayashi, M. Tomita, T. Yoshimura, Nucleotide sequence of genome segment 5 from bombyx mori cypovirus 1, Arch. Virol. 146 (1) (2001) 181–187.
[27] C. Han, E. Chen, G. Shen, Z. Peng, Y. Xu, H. Zhang, H. Liu, Y. Zhang, J. Wu, Y. Lin, et al., Vitellogenin receptor selectively endocytoses female-specific and highly-expressed hemolymph proteins in the silkworm, bombyx mori, Biochem. Cell Biol. 95 (4) (2017) 510–516.
[28] R. Li, C. Hu, T. Geng, D. Lv, K. Gao, X. Guo, C. Hou, Expressional analysis of the silkworm storage protein 1 and identification of its interacting proteins, Insect Mol. Biol. 29 (1) (2020) 66–76.
[29] S. Kim, S.K. Hwang, R.A. Dwek, P.M. Rudd, Y.H. Ahn, E.-H. Kim, C. Cheong, S.I. Kim, N.S. Park, S.M. Lee, Structural determination of the n-glycans of a lepidopteran arylphorin reveals the presence of a monoglucosylated oligosaccharide in the storage protein, Glycobiology 13 (3) (2003) 147–157.
[30] B. Stiles, Cuticle proteins of the boll weevil, anthonomus grandis, abdomen: structural similarities and glycosylation, Insect Biochem. 21 (3) (1991) 249–258.
[31] M. Wiedmann, T.V. Kurzchalia, E. Hartmann, T.A. Rapoport, A signal sequence receptor in the endoplasmic reticulum membrane, Nature 328 (6133) (1987) 830–833.
[32] Y. Takada, X. Ye, S. Simon, The integrins, Genome Biol. 8 (5) (2007) 215.
[33] Y. Zhang, G. Cao, L. Zhu, F. Chen, M.S. Zar, S. Wang, X. Hu, Y. Wei, R. Xue, C. Gong, Integrin beta and receptor for activated protein kinase c are involved in the cell entry of bombyx mori cypovirus, Appl. Microbiol. Biotechnol. 101 (9) (2017) 3703–3716.
[34] J. Li, L. Ma, Z. Lin, Z. Zou, Z. Lu, Serpin-5 regulates prophenoloxidase activation and antimicrobial peptide pathways in the silkworm, bombyx mori, Insect Biochem. Mol. Biol. 73 (2016) 27–37.
[35] M.S. Kolodney, E.L. Elson, Contraction due to microtubule disruption is associated with increased phosphorylation of myosin regulatory light chain, Proc. Natl. Acad. Sci. U. S. A. 92 (22) (1995) 10252.
[36] S. Takashima, Phosphorylation of myosin regulatory light chain by myosin light chain kinase, and muscle contraction, Circ. J. 73 (2009) 208–213.